3.5 NEAR SURFACE TURBULENCE FORECASTING CHALLENGES:

PROGRESS IN TRAPPED WAVE FORECASTING AT THE

UNITED STATES AIR FORCE WEATHER AGENCY

James R. McCormick*

University Corporation for Atmospheric Research, located at Offutt AFB, Nebraska

1. Introduction

Turbulence forecasting remains a significant concern for the United States Air Force Weather Agency (AFWA). Turbulence continues to prove threatening to the safety of passengers and cargo. Trapped waves often prove to be regions of enhanced turbulence threat and enhanced turbulence severity. At the current time, very little is available in terms of operational forecast products for aviation interests. This research attempts to meet this need of aviation forecasters by identifying meteorological features common to trapped wave events, and producing operationally-effective products based on the numerical model resources available.

2. Motivation

Trapped waves are known regions where risk of atmospheric turbulence is enhanced. The severity of turbulence is also likely to be enhanced in these regions.

At the current time, few products are made available to operational forecasters to aid in the process of forecasting trapped waves. Current AFWA operations include methods for forecasting the development of mountain waves, but do not include forecast propagation techniques, though turbulence caused by trapped mountain waves can extend many miles east of the terrain gradient. In addition, little exists in terms of forecast product for other trapped waves, such as gravity waves. These waves are a particular problem within the boundary layer when reflected wave energy can then be reflected and trapped by the ground, and currently, the Panofsky Turbulence Index, which is used for near-surface turbulence forecasting, is not designed to capture turbulence created by mesoscale waves.

The goal of this research is to create practical, operationally effective indicators of trapped wave potential, and to format these products into probabilistic form to convey the potential and uncertainty of expected conditions. It is not in the design of this project at this state to differentiate between types of trapped waves – merely to attempt to forecast areas were any type of wave trapping is preferred.

3. Methodology

3.1. Model Detail

AFWA has recently completed a transition to 15 KM WRF data for nearly all domains globally, upgrading from previously run MM5 forecasts. Some areas of higher resolution, such as 5 KM resolution, are available for smaller domains. Because these domains are not available for every location, the 15 KM data is chosen so that products may be implemented for nearly any location of interest.

AFWA operations version 3.2 of the WRF, nested within a 45 KM domain, and uses 3DVAR data assimilation. The grid is 343 X 211, spaced at 15 KM horizontal resolution, and contains 56 vertical levels. Data is output at 3-hour time steps out to 48 hours.

The CONUS domain is chosen for the evaluation and development portion of this study because of high resolution satellite data, as well as several other sources of data (including radar, surface observations, upper air soundings, and wind profilers) that enable us to best study

- *Corresponding author email address*: James.McCormick.Ctr@offutt.af.mil

atmospheric features. Calculations are made using sigma data for multiple reasons. Of the most important reasons are that sigma level data provides more vertical resolution than standard levels, and that sigma levels allows for a better handle in areas of significant terrain.

3.2. Challenges

As with almost any turbulence forecasting project, numerous challenges are faced when attempting operational trapped wave forecasting and deciphering turbulence caused by trapped waves.

The verification of the existence of waves and turbulence is considered to be a non-trivial limitation. The limitations of pilot reports are well documented (for example, Brown and Young 2000). In addition, turbulence may be the result of any one of several different processes, and it is not within our abilities to specifically determine, in all cases, the specific atmospheric process which causes turbulence.

Even the simple identification of waves presents challenge. Trapped waves are subjectively identified using visible satellite imagery. The author needed to feel confident that the cloud patterns were the result of a wave, without the possibility that the clouds were the result of another feature, such as a horizontal convective roll, before placing the wave into the study. Also, higher clouds often times obscured the existence of a wave in a given region. For verification purposes for this study, if no wave could be proven using satellite data, no wave was considered to be present, but that does not mean that no wave was present in the area.

Limitations within the operational model also provide significant challenges. Within the 15 KM WRF model, varying vertical resolution changes with height, making uniform calculations impossible. It is of particular note that as height increases and the depth of vertical layers becomes deeper, it becomes more difficult to specifically identify where a small scale feature is present. Considering that reflecting layer features that are of interest may often exist within a small vertical layer of only a few meters, it becomes increasingly difficult to pinpoint the location of a specific layer within the model. In addition, calculations are often dampened within deeper layers, making it harder to discern which grid points contain data of particular use and which grid points do not, even if the values for the layer end up being the same. A gentle wind shift over the course of 600 meters will not produce the same effect as an abrupt shift over 50 meters within a 600 meter layer, for instance. However, there is no way within the limitation of the 15 KM WRF model to tell the difference.

With these challenges in mind, it is still useful to identify regions where conditions are noted to be favorable for trapped waves – the 15 KM horizontal resolution and 3 hourly time steps provide sufficient detail of wind and temperature data to identify mesoscale environmental features, if not the waves themselves, and these details will be discussed in the next section.

4. Product Development and Consideration

4.1. Model Indicated Vertical Velocities

Recent work within AFWA (Keller 2011) has strongly suggested that the 15 KM WRF can detect vertical velocities associated with mountain waves. Horizontal cross sections of vertical velocities were created from data across a portion of northern Nevada for a trapped wave case on 6 June 2011 [Figure 1].

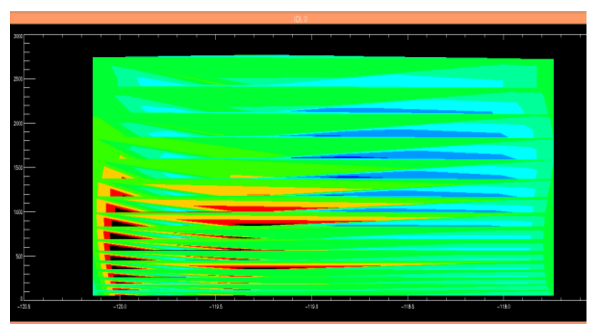

Figure1: Color coded vertical velocities from a horizontal cross section across northern Nevada for a trapped mountain wave case, 6 June 2011.

Warm colors indicate rising motions; cool colors indicate descending air. The wave-like structure is only noted below approximately 1500 m, which agrees with a significant area of curvature in the 00Z REV sounding [Figure 2].

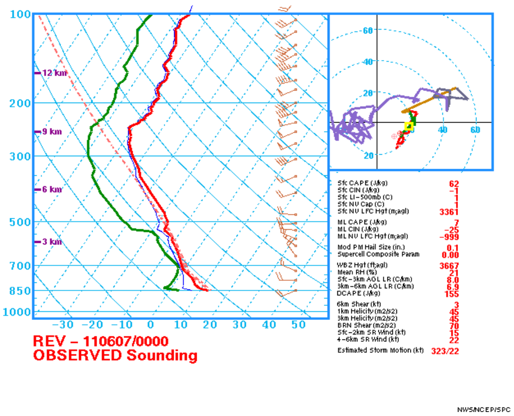

Figure 2: 00Z REV Sounding 7 June 2011

Another method of data display was the comparison of plots of vertical velocities from the lowest 10 sigma levels (which contain data to approximately 1500 m AGL) with plots of vertical velocities from the lowest 17 sigma layers (which contains data to approximately 4000 m AGL) [Figures 3a, 3b].

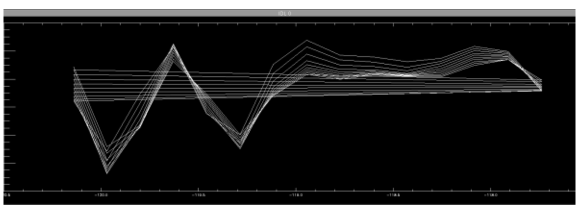

Figure 3a: 10 layer vertical velocities, horizontal cross section across northern Nevada, 6 June 2011

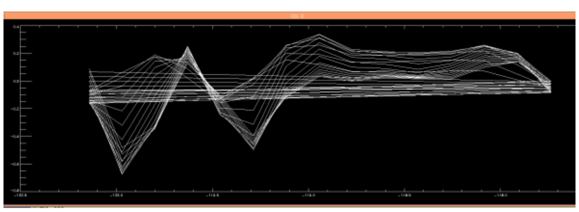

Figure 3b: 17 layer vertical velocities, horizontal cross section across northern Nevada, 6 June 2011

In Figure a, a strong harmonic wave structure is noted, while in Figure b, with the introduction of data from higher levels, the signal becomes softer, indicating that the strongest wave motions were being forecast within the lowest 1.5 km of the atmosphere.

Such examples as 6 June 2011 gave encouragement in that specific layers of interest where waves were occurring could be identified, and that these levels could be identified within the model. However, because not all waves are going to be of a necessary size to show up in 15 KM data, and other waves will not be forecast at all, efforts remains focused on forecasting environmental conditions surrounding trapped waves, and not specifically looking for the waves themselves within the model data.

4.2. Scorer Parameter

Traditional trapped wave forecasting often references the Scorer Parameter (Scorer 1948), an equation that takes into account thermodynamic and dynamic properties of the atmosphere, as well as considerations of the properties of the trapped wave.

The Scorer Parameter, l^2, is given by:

$$(1)\quad l^2 = \frac{N^2}{(c-U)^2} - \frac{dU^2}{(c-U)*d^2z}$$

Where N^2 represents the Brunt Vaisala frequency given by

$$(2)\quad N^2 = \frac{g}{T_V} * \frac{\Delta\theta_V}{\Delta z},$$

c represents the phase speed of the wave, U represents the mean wind vector for a given layer. (For mountain waves, U is sometimes represented as the terrain-perpendicular mean wind flow.) T_v represents virtual temperature, and θ_v represents virtual potential temperature. For the purposes of this paper and ease of discussion and display, all Scorer Parameter values are scaled by a factor of 10^4 unless otherwise noted.

Graphical displays of Scorer Parameter were created, such as for a case on 25 August 2011 [Figure 4].

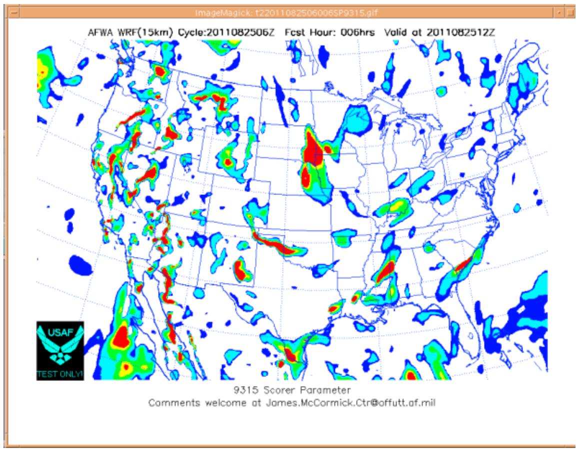

Figure 4: 25 August 2011: Scorer Parameter at the 9315 Sigma Level

Scaling was created after study of numerical output indicated that Scorer Parameter values on the order of -1 or lower were found in instances of trapped waves. On this particular date, a trapped wave was clearly visible on satellite imagery in the northeastern United States. While the Scorer Parameter correctly identified a region of heightened potential in New England, it also highlighted several areas throughout the western United States where no waves were noted. It is worth noting at this point that just because no evidence of a wave was seen, that does not mean that no waves were present. However, what was noted was that the particular region of interest was not specifically highlighted by the Scorer Parameter image. To quantify this subjective analysis, data from grid points from within the geographical region of the wave were examined individually. One grid point was located near Auburn, Maine, and contained a Scorer Parameter value of

-1.3646. This value only ranked in the top 28.5% of all values within the domain, and as such, provides very little, if any, discriminating information for an operational forecaster. Another grid point, located near Millinocket, Maine, had a Scorer Parameter value of -2.0023, which ranked in the top 12.4% of all values within the CONUS domain. While this result was better, it still meant that areas in New England were not distinguishable from several other regions within the domain. Other grid points were examined throughout the wave region, with no appreciably better results noted. Meanwhile, throughout regions where the Scorer Parameter values were the lowest, no noticeable wave patterns were detected.

With a recognition that the Scorer Parameter results vary slightly with respect to the differing depths of vertical layers, the following probability of detection statistics have been calculated:

1) SP < 0: 1.0000
2) SP < -1: .9565
3) SP < -2: .8696
4) SP < -3: .4348
5) SP < -5: .2174
6) SP < -7.5: .1304

In order to determine how well the Scorer Parameter specified regions of trapped waves for individual charts, grid points within known waves were compared to all grid points for the respective chart.

1) SP @ top 25%: .8696
2) SP @ top 15%: .7391
3) SP @ top 10%: .3478
4) SP @ top 5%: .2174
5) SP @ top 1%: .0000

While negative values of the Scorer Parameter are noted in nearly every trapped wave case, it is not clear that the values depicted within these environments are particularly specific for the end user. This result is not to be considered to be any sort of indictment against the Scorer Parameter – it is simply a suggestion that the limitations of the operational models preclude accurate and specific determinations of trapped wave locations using the Scorer Parameter. For some cases, the Scorer Parameter works quite well, particularly displayed as a vertical profile (used as a valuable method for displaying atmospheric characteristics in other works (Grubišić and Billings 2007)), such as the case of 14 April 2011 in New York [Figure 5]. Figure 5 shows a vertical profile of the Scorer Parameter (unscaled) with respect to height, and very clearly shows a local minimum of approximately -5 near 1000 m.

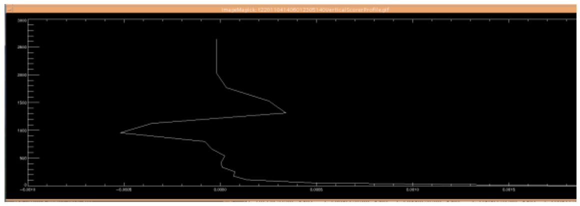

Figure 5: 14 April 2011 Scorer Parameter (unscaled) vertical plot, located in New York state

Because of the previously mentioned computational difficulties with the Scorer Parameter, however, attempts were made to determine what physical properties represented by equations such as the Scorer Parameter were particularly well defined within the limitations of our operational model.

4.3. Wind Shear Parameterization

As noted in both terms of the Scorer Parameter, wind shear is a particularly important term in the Scorer calculation. Several examples have been noted of strong wind shear in atmospheric wind profiles near a trapped wave, and the theory of wind curvature playing a significant role in the existence of a wave duct is well noted in literature (Nappo 2002, Coleman et al 2009, as well as many others).

Attempts to parameterize the wind shear were based on these cases, with cases of unidirectional wind shear also noted to be present during a strong trapped wave case [Figure 6] if the shear was strong.

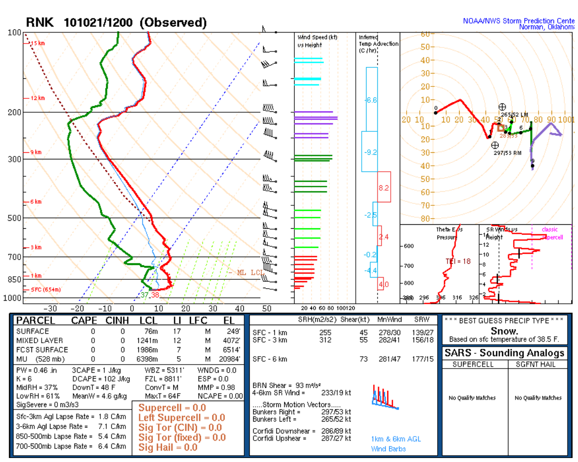

Figure 6: 21 October 2010 RNK sounding associated with intense trapped mountain wave that resulted in severe turbulence reports in the Washington DC metro area

15 KM WRF data directly outputs values for the u- and v-components of wind flow. It was quickly recognized that some combination of u- and v-component change could be noted in soundings and profiler data near trapped wave events. Computations of du/dz (dv/dz) for a given sigma level are made by subtracting the u- (v-) component of the level above the sigma layer of interest from the u- (v-) component of the level below the sigma layer of interest. This result is divided by the distance between the two layers. For example, du/dz (9645) = u(9550) – u(9735)/z(9550) – z(9735).

It was also likely that the likelihood of a trapped wave increased exponentially as the change in the u- and v- components. The du/dz and dv/dz terms are squared, which give terms that will be called DU2 and DV2 for the rest of this paper.

First attempts to use this idea operationally simply represented an attempt to add the DU2 and the DV2 terms together, with a minimum value of 10 m^2/s^2 for each term. Though this calculation quickly proved to not be a sufficient method of capturing trapped waves, one gravity wave in northwest Missouri was captured, with specificity, by this forecast [Figure 7].

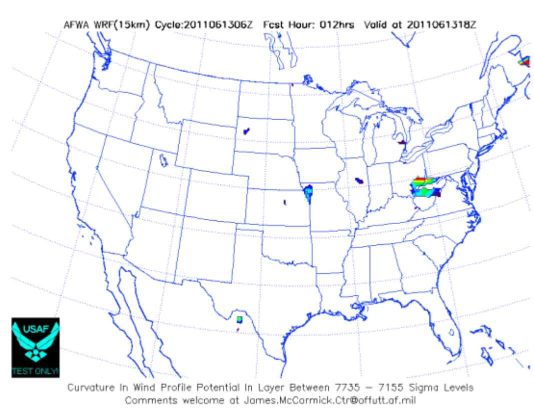

Figure 7: Wind Shear Term (early formula);

13 June 2011

Adding to confidence in this product was the fact that multiple pilot reports were received from the particular region of moderate turbulence. Radar review indicated that all precipitation cores were located at least 100 km to the east, giving the appearance that the gravity wave was the most likely cause for this particular turbulence.

It became quickly apparent that strong minimum thresholds were going to eliminate environments that were favorable for wave trapping. Minimum thresholds were lowered to 6 m2/s2 for each term, and then each term was multiplied together, placing greater emphasis on cases where both terms had a significant change. Eventually, through further study, it was noted that any change where the DU2 term multiplied by the DV2 term was greater than 1 may result in a favorable environment for wave trapping, and that particularly for lower layers, this threshold did not result in extraneous forecast coverage. For levels above approximately 2000 m, a higher DU2 * DV2 threshold will be needed due to the decreased vertical resolution in the model.

For the 25 August 2011 case, the same grid points were examined as in section 4.1. The grid point near Auburn, Maine, noted a wind shear value of 38.5, which ranked amongst the top 4.5% of all values within the grid. The grid point near Millinocket, Maine, noted a value of 219.5, which ranked amongst the top 1.1% of all values within the CONUS domain. The graphical display of level of interest is given below [Figure 8], which shows a clear focus upon the northeastern United States, as well as upon Hurricane Irene east of Florida.

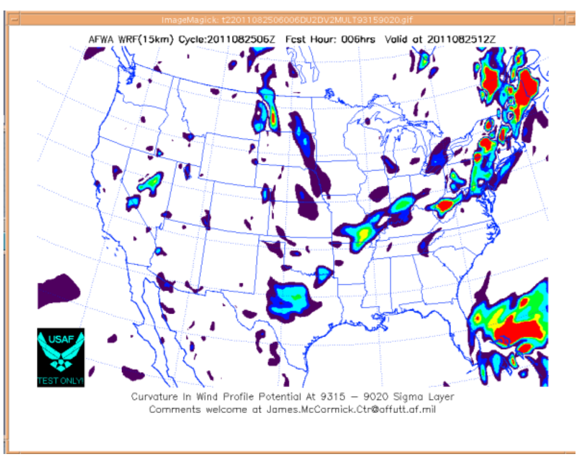

Figure 8: 25 August 2011 Wind Shear Term

Sigma Layers: 9315-9020

For verification purposes, specific thresholds used for plotting purposes are used as measures for probability of detection at each level:

1) DU2*DV2 @ 1: 1.0000
2) DU2*DV2 @ 25: .8696
3) DU2*DV2 @ 50: .7391
4) DU2*DV2 @ 100: .6522
5) DU2*DV2 @ 250: .3043
6) DU2*DV2 @ 500: .0870

Also, similar to methodology used for the Scorer Parameter, the probability of detection for specific chart-based thresholds have been computed.

1) DU2DV2 @ 25%: 1.0000
2) DU2DV2 @ 15%: .9565
3) DU2DV2 @ 10%: .9565
4) DU2DV2 @ 5%: .8261
5) DU2DV2 @ 1%: .3043

Vertical profiles of the wind shear term also have been created, allowing a user to visualize the location of reflecting layers for a given point [Figure 10].

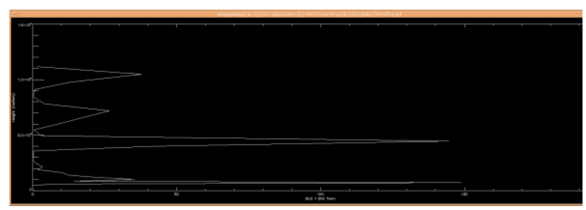

Figure 10. Vertical plot of wind shear term,

1 September 2011, northern Wisconsin.

A significant advantage to the use of vertical plots is that if multiple reflecting layers are present in an atmosphere, or if one layer is particularly dominant, the user can see all potential reflecting layers, at least at the resolution that the model will allow. For the case of 1 September 2011 in Wisconsin, noted in Figure 10, a significant low level trapping layer was present, while a mid level trapping layer was present as well. Satellite imagery indicated both low- and mid-level wave trapping in northern Wisconsin.

Using the raw data for given points can also allow a user to focus on trends . For a small trapped wave case in Utah on 8 July 2011 [Figure 11], a mountain wave that formed in the morning over a ridge near the AZ/UT border dissipated as the day went on.

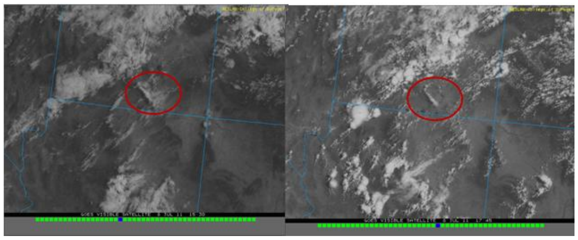

Figure11: 1530Z and 1830Z visible satellite data, courtesy of the College of DuPage weather lab (http://weather.cod.edu), showing a small trapped wave in southern Utah at 1530Z, no longer present at 1830Z.

Wind shear data for the 5120 level at 15 Z was recorded as 147.0 for a grid point located in southern Utah; at 18 Z that value had dropped to 4.5. For the 4760 sigma level,15 Z data indicated a value of 244.3, while the 18Z data indicated a value of 6.7. While conditions still remained possible for trapped waves in the region, the likelihood had dramatically decreased based on the decrease in wind shear values in the 3-hour time step.

With a limited dataset so far, wind shear has noted in almost every trapped wave case to be more specific in discriminating trapped wave locations than the Scorer Parameter. The average Scorer Parameter rank is within the top 12.5% of all data for each respective grid; the average wind shear term rank is within the top 3.1% of all data for each respective grid. Subjective analysis of graphical displays have also been performed as part of this examination to ensure that maximum grid point values are studied, and that results are not skewed by small geographical errors within the model data. It is also understood that a limitation of this data set is that these data are products of the trapped waves observed and studied in the summer of 2011 within the CONUS domain, and may not be entirely representative of trapped waves in general. What has been noted so far is that the 15 KM WRF does seem to do an excellent job of forecasting existing wind shear, at least within the 6-18 hour forecast period. More investigation of longer range forecasts (21-48 hour forecasts) is needed to determine how successful these forecasts are at longer ranges.

5. Summary And Conclusions

Trapped wave forecasting continues to prove to be a substantial challenge. The 15 KM WRF being utilized for operational forecasts at the United States Air Force Weather Agency shows some good results in being able to forecast areas of wind shear associated with reflecting layers able to trap waves, but is not as successful when attempting to identify regions where thermodynamic profiles play a key role in the creation of a wave duct.

When identifying regions of known trapped waves, using a parameterized wind shear term appears to be a very good discriminator of the local environment when compared to local climatology and surrounding areas. The author acknowledges the possibility that the Scorer Parameter may perhaps indicate more regions where reflection is possible, but without direct evidence of waves in many of these areas, it is impossible to specifically quantify the use of this parameter operationally.

6. Future Work

Trapped wave forecasting continues to provide a substantial challenge.

Work will continue to tweak the wind shear formula. Weaknesses are noted with the lack of a uniform distribution of vertical levels. What is considered strong wind shear at a sigma layer low in the atmosphere may not be sufficient to create a reflecting layer in a sigma layer high in the atmosphere. It is also impossible to note if a sufficient wind shear value occurs gently throughout a layer in the upper atmosphere, which also may not be sufficient to create a reflecting layer. Dampening coefficients based on thickness of the layer of interest have been discussed and are the most likely implementation to address this issue.

It is noted that not all trapped waves produce turbulence. Since turbulence, particularly moderate or greater (MOG) turbulence, is the key atmospheric feature of interest for AFWA, and not simply the presence of these trapped waves, work will need to be done to discriminate between benign trapped waves and MOG turbulence-producing trapped waves.

It is also not the intention of this paper to ignore the thermodynamic contribution to wave ducting, as noted in several case studies (Adams Selin 2011, Ruppert 2011, and many others). Theories put forth in literature (Lindzen and Tung 1976, Koch and O'Handley 1997, and others) will continue to be studied, and attempts to parameterize thermodynamic wave ducting will continue.

Emphasis continues to be placed on probabilistic forecasting methods within AFWA. The goal of this effort is to rely less on deterministic thresholds and more on the likelihood of an event based on numerical data.

Probabilistic based results also provide numerical output for the ensembles team within the 16th Weather Squadron to more easily use. Ensembles based forecasting will allow for the consideration of a variety of numerical solutions, and stamp charts allow a user to see multiple potential solutions in advance, consider these potential solutions, while making a more final determination as the event unfolds.

7. Acknowledgments

The author would like to extend his sincerest thanks to Cpt. Paul Lucas, David Keller, Evan Kuchera, Rebecca Adams-Selin, and Scott Rentschler of the 16th Weather Squadron within AFWA for their valuable contributions and considerations within this work. In addition, the author would also like to thank Dr. Clark Evans of the University of Wisconsin-Milwaukee, Dr. John Knox of the University of Georgia, and James Ruppert of Colorado State University, for discussions regarding operational trapped wave forecasting. Finally, the author thanks UCAR and Northrop Grumman for the financial support for this project and for the opportunity to present the research from this project.

8. References

Adams-Selin, R.D., 2011: Examination of atmospheric waves associated with 13 March 2003 bow echo. *15th Conference on Mesoscale Processes*, Los Angeles, Amer. Meteor. Soc.

Brown, B.G., and G.S.Young, 2000: Verification of icing and turbulence forecasts: why some verification statistics can't be computed using PIREPs. *9th Conference on Aviation, Range, and Aerospace Meteorology*, Orlando, Amer. Meteor. Soc.

Coleman, T.A., K.R. Knupp, and D. Herzmann, 2009: The spectacular undular bore in Iowa on 2 October 2007. *Mon. Wea. Rev*., **137**, 495-503.

Grubišić, V., and B.J. Billings, 2007: The intense lee-wave rotor event of Sierra Rotors IOP 8. *J. Atmos. Sci.*, **64**, 4178-4201.

Keller, D., 2011: Semi-emperical methods for the prediction of mountain wave turbulence. *14th Conference on Aviation, Range, and Aerospace Meteorology*, Los Angeles, Amer. Meteor. Soc.

Koch, S.E., and C. O'Handley, 1997: Operational forecasting and detection of mesoscale gravity waves, 1997. *Wea. Forecasting*, **12**, 253-281.

Lindzen, R.S., and K.K. Tung, 1976: Banded convective activity and ducted gravity waves. *Mon. Wea. Rev.*, **104**, 1602-1617.

Nappo, C.J., 2002: *An Introduction to Atmospheric Gravity Waves.* Academic Press, 276 pp.

Ruppert, J., 2011: A case study of a large-amplitude mesoscale inertia-gravity wave over the southeast US. *15th Conference on Mesoscale Processes, Los Angeles*, Amer. Meteor. Soc.

Scorer, R.S., 1948: Theory of waves in the lee of mountains. *Quart. J. Roy. Meteor. Soc*., **75**, 41-56.